Reducing ageing of thin PTMSP films by incorporating graphene and graphene oxide: Effect of thickness, gas type and temperature

19 April 2024

Author's Accepted Manuscript

Reducing ageing of thin PTMSP films by incorporating graphene and graphene oxide: effect of thickness, gas type and temperature

Luca Olivieri, Silvia Meneguzzo, Simone Ligi, Andrea Saccani, Loris Giorgini, Alessandro Orsini, Alberto Pettinau, Maria Grazia De Angelis

Cite this article as: Luca Olivieri, Silvia Meneguzzo, Simone Ligi, Andrea Saccani, Loris Giorgini, Alessandro Orsini, Alberto Pettinau and Maria Grazia De Angelis, Reducing ageing of thin PTMSP films by incorporating graphene and graphene oxide: effect of thickness, gas type and temperature, *Journal of Membrane Science,* https://doi.org/10.1016/j.memsci.2018.03.056

Reducing ageing of thin PTMSP films by incorporating graphene and graphene oxide: effect of thickness, gas type and temperature

Luca Olivieri[a], Silvia Meneguzzo[a], Simone Ligi[b], Andrea Saccani[a], Loris Giorgini[c], Alessandro Orsini[d], Alberto Pettinau[d], Maria Grazia De Angelis[a*]

[a]Dipartimento di Ingegneria Civile, Chimica, Ambientale e dei Materiali (DICAM), Università di Bologna, Via Terracini 28, 40131 Bologna, Italy.

[b]Graphene XT s.r.l., Via Massimo d'Azeglio 15, 40131 Bologna, Italy.

[c]Dipartimento di Chimica Industriale "Toso Montanari" Università di Bologna, Viale Risorgimento 4, 40136 Bologna, Italy.

[d]Sotacarbo SpA, Grande Miniera di Serbariu, 09013 Carbonia, Italy

* Corresponding author. E-mail: grazia.deangelis@unibo.it

ABSTRACT

It was previously proven that small loadings of few-layer graphene (G) and monolayer graphene oxide (GO) adjust the permselectivity and reduce the ageing of thick poly(trimethyl silyl propyne) (PTMSP) membranes, which currently inhibits their application in real separations. In this work, we extend the analysis to thin film composite membranes with top layers of PTMSP/G and PTMSP/GO between 1 and 7 micrometers. The good quality of the films, obtained by spin coating the polymer solution on porous flat supports, indicates that graphenic sheets are aligned parallel to the film surface, without defects, and that the large-scale production of such composite films is feasible. The addition of G and GO to PTMSP can improve the gas permeability and selectivity, and even change the behaviour from CO_2-selective to He-selective. GO produces more repeatable effects than graphene, and it generally enhances the PTMSP permeability.

The ageing was studied by tracking permeability of 4 gases with time: thin films age faster than thick ones, because ageing is due to free volume diffusion across the film. Incorporation of 1 wt% of G and GO visibly reduces the ageing of thin PTMSP films, and the effect is repeated on many different samples. The ageing can be correlated, with a single power law, to the ratio between time and squared film thickness. The exponent of such function, that quantifies the ageing rate, decreases when G and GO are added to PTMSP thin films, by factors as high as 40%.

The temperature effect was studied, up to 60°C, on annealed samples: the membranes, CO_2-selective at room temperature, can become easily He-selective by raising the temperature. The He/CO_2 selectivity increases with temperature: such effect could be exploited syngas purification and pre-combustion capture processes.

Keywords: PTMSP; graphene; ageing; gas separation; thin films.

1. Introduction

The gas separation performance of high free volume glassy polymers, such as the polymer of intrinsic microporosity (PIM-1), or poly(trimethyl silyl propyne) (PTMSP) lies very close to the Robeson's upper bound that limits size-sieving membranes for several gas couples, in the region characterized by high permeability and low selectivity.[1] To improve the performance of such materials, one can adopt various strategies, such as incorporating inorganic fillers to form Mixed Matrix Membranes, MMMs.[2-13] The inorganic fillers may be porous and selective, or dense and impermeable. In the latter case, especially when they are in the form of nanospheres, inorganic fillers usually have a good morphological compatibility with high free volume glassy polymers, and tend to adjust the chain packing of polymers in a way that affects positively the permselectivity, without creating non selective voids.[14] When the porous, selective fillers are added, the combination of the intrinsic selective performance of matrix and dispersed phase can lead to synergetic effects which improve the permselectivity. [15-16]

In both cases, the most challenging step in the fabrication of industrially relevant mixed matrix membranes is the ability of producing thin films, of the order of 1 micrometer and less, depending on the polymer permeability, without defects and pinholes. To do so, the dispersed phase must be well distributed inside the polymer, have a characteristic size not exceeding the thickness of the film, and, when in the form of a flake, align parallel to the surface to avoid any defect.

Furthermore, when the high free volume glassy polymers are considered, one aspect that must be kept under control is the ageing: indeed, while showing excellent permeability performance soon after casting, the properties of such materials tend to worsen with time, due to shrinking of free volume.[17-18] It has been observed also that ageing rate of thin films is a function of film thickness.[19-21] In particular for thicknesses in the range of several micrometres up to millimetre scale, the ageing rate is independent on thickness; this is the case of so called bulk films for which it is expected that properties are independent on film thickness. For films with thickness in the range from 100 nm up to few micrometres, which is the range of interest for membrane applications, it is

2

possible to observe that the ageing rate increases by decreasing the film thickness. Such effect has been observed in particular in PTMSP. [21]

The effect that the filler has on the polymer tendency to age must be accurately characterized: indeed, some fillers pose a constraint to the polymer free volume relaxation and inhibit ageing. Literature studies evaluated the reduction of ageing obtained by adding different particles to glassy polymers, such as functionalized carbon nanotubes to PIM-1,[22] or by micro particles of porous aromatic frameworks (PAF) to different glassy polymers.[23] Kelman *et al.* showed that poly siloxysilsesquioxanes (POSS) nanoparticles lower the ageing of PTMSP, but reduce its permeability.[24] Matteucci *et al.* found that addition of TiO_2 nanoparticles up to 20 vol% reduces the physical ageing of PTMSP, while the same amount of MgO particles does not affect it. A fairly large volume fraction (75%) of MgO is required to reduce ageing of PTMSP. [25-26]

Recently, a new class of inorganic material has been evaluated successfully for application in membrane-based gas separations, namely graphene (G) and its derivatives, such as graphene oxide (GO).[27-32] While a defect-free graphenic layer is virtually impermeable to all molecules,[33] some production techniques may introduce a microporosity, which make it permeable to gases. Furthermore, when the graphene is added in subsequent layers, permeable channels caused by imperfect adhesion between the layers may form. Graphene Oxide, on the other hand, naturally contains defects induced by the oxidation process, and is endowed with an intrinsic gas permeability and selectivity.[34] Kim and coworkers prepared ultrathin GO membranes on a polyethersulfone (PES) support membrane, obtaining selective transport of CO_2 over hydrogen, methane and nitrogen in the presence of water vapor.[35] Li *et al.* showed that structural defects on molecular sieving GO membranes provided highly H_2 permeation over CO_2 and N_2.[28] Shen *et al.* reported a methodology that involves GO assembly in polymeric environment, yielding well-defined GO laminates in which the interlayer spaces could provide molecular sieving channels of the size of 0.35 nm.[36] The CO_2 permeability reached 100 Barrer and CO_2/N_2 selectivity was 91,

3

breaking the permeability/selectivity trade-off relation in polymeric membranes. Recently Li et al, considered the combination of carbon nanotubes, CNTs, and GO nanosheets in commercial polyimide Matrimid®.[37] They observed that an optimal formulation was 5% of GO and 5% of CNTs content, which led to an increase of free volume cavity size and enhancement in CO_2 permselectivity. Similarly, a GO/polyimide (PI) mixed matrix membrane was fabricated by in situ polymerization of PI precursors and GO with different oxidation degrees. The optimal formulation in this case resulted to be 1 wt% with simultaneous maximization of CO_2 permeability and CO_2/N_2 selectivity.[38]

Another group of researchers studied the combination of graphene, obtained by in situ exfoliation of graphite in polymeric solution, to PIM-1. The studies indicate that an optimal concentration of graphenic filler is equal to 0.1 wt%, as such amount allows to maximize the CO_2 permeability of PIM-1. Ageing studies indicate an ageing rate comparable for the neat PIM-1 and the composite PIM-1 membrane, while simulations indicate that the presence of graphene layers affects the polymer distribution.[39-41]

In a previous work, we demonstrated the ability of graphene-based filler, added in solution, to influence PTMSP permselectivity and physical ageing on films of the order of 100 micrometers. [42] In particular, the experiments showed that the addition of 1 wt% of monolayers of GO (lateral dimension 2 μm, thickness 1.1 nm) slightly enhances the gas permeability of PTMSP, and the selectivity for the couple CO_2/He and CH_4/He. The solubility and diffusivity are both enhanced by addition of GO filler. The addition of a few layer graphene (lateral dimension 5 μm, thickness 2-8 nm) in the same amount to PTMSP lowers slightly the gas permeability, with factors that increase with decreasing molecule size, and enhances the ideal selectivity for the couples CO_2/He and CH_4/N_2, CH_4/He. The addition of this filler mainly lowers the diffusivity, leaving the gas solubility unaltered. Multiple layer graphene (lateral dimension 0.2 μm, thickness 2-20 nm) lowers the

4

permeability of PTMSP to a significant extent (up to -30%), even though their fraction is only 1 wt%.

The most interesting results of that work, however, regards the effect of filler addition on the ageing behavior of PTMSP. In particular, the addition of GO and few-layer graphene slows down the ageing process, tracked with He, N_2, CH_4 and CO_2 permeability. Such effect is durable, as also the final, pseudoequilibrium CO_2 permeability value attained after annealing at 200°C under vacuum is higher for PTMSP/GO than for PTMSP membrane. The reduction of PTMSP ageing observed is higher than that obtained in the literature with the use of other fillers as TiO_2 and MgO, even though the amount of filler added in this case is much smaller. The effects were attributed to the fact that graphene platelets, due to their high aspect ratio, act as physical barriers to the redistribution of polymer chains, and the diffusion of free volume pockets, which cause the ageing. Such explanation is confirmed by the fact that ageing is mostly reduced by the fillers that have the higher initial aspect ratio, while no effect is observed with the multi-layer graphene, that is characterized by a lower aspect ratio. The shape effect is important, as it was also indicated by other groups studying the effect of fillers of different curvature, namely nanospheres of silica, nanotubes of carbon and nanosheets of graphene- in PIM-1. Such authors indicated that the smaller the filler curvature, the larger the effect that the filler has on the chain packing and, ultimately, on the permselectivity of polymer.[40] When different graphenic fillers are considered, the curvature is similar, although graphene oxide is less flat then graphene, and the shape of the material relates directly to the aspect ratio, i.e. the ratio between lateral size and thickness. It must be noticed that treatments like sonication, required to have dispersion of graphene in the polymer solution, can reduce the aspect ratio, and that the sonication yields scarcely reproducible effects. Indeed, it was proven that the sonication of graphene oxide platelets can reduce significantly their aspect ratio. [43,44]

In the present work, we tested the scalability of the mixed matrix membrane synthesis procedure by fabricating thin film composite membrane formed by porous polymeric supports and thin (1-7 μm)

layers of PTMSP, PTMSP/G and PTMSP/GO via a spin coating technique. The attainment of defect-free membranes is essential for the industrial application of such membranes, and could provide a proof that the graphenic platelets, whose initial lateral size ranges between 2 and 5 μm, align parallel to the membrane surface by the shear flow attained during the spin coating process. Shear-induced alignment of GO was indeed already observed when coating porous polymeric hollow fibers of with a composite PEBAX/GO thin film, via the dip coating technique.[45]

The testing of gas permeability and ageing rate on thin films, serves also to check the reproducibility and applicability of PTMSP/G and PTMSP/GO mixed matrix membranes. Indeed, since PTMSP films in the micrometric range tend to age much faster than thicker samples, an ageing test carried out on thin films is much more stringent than one carried out on thick membranes.

2. Experimental

2.1. Preparation of solutions

PTMSP was purchased by Gelest, and chloroform (purity > 99.5% Sigma Aldrich) was used as solvent. The graphenic based fillers were provided by Graphene XT. The graphene (G) used is a few layer graphene with lateral dimension of 5 μm and thickness of 2-8 nm, 2% wt. of undisclosed dispersing agent and an oxygen content close to 1%. The SEM images of the Graphene used, dry and in water solution, can be viewed in a previous work.[46] The graphene oxide (GO) used was dried from a commercial solution with nanoplatelets with lateral sheet dimension of 2 μm and thickness of 1.1 nm, a monolayer content higher than 95% and C/O mass ratio equal to 1.

Solutions were prepared dissolving the PTMSP in chloroform to obtain 1 wt% solution, and adding the filler in percentage of 1% with respect to the mass of the polymer. The solution was sonicated for 5 hours to reach a stable dispersion of platelets: during such step the size of the graphenic platelets may decrease with respect to the initial value. Finally, before the deposition, the solutions

6

were evaporated in the bottles to reach half of the initial volume and increase their initial viscosity, so to hinder sedimentation of graphenic nanoplatelets during casting.

2.2. Preparation of thin film composite membranes

Thin membrane were fabricated using the spin coating technique, according to the procedure depicted in **Figure 1**. This instrument allows to obtain a thin and homogeneous layer of polymer, due to its high rotational speed. The polymer solution was spread on a polypropylene support. A commercial porous (37%) polypropylene (Celgard®) film of about 25 μm (with pore size of 0.117 μm x 0.042 μm) was used. The porous support was fixed on the spin coater at a speed of 2000 rpm, then two injections of 200 μL of polymer solution were performed, at time intervals of about one minute from each other.

After the deposition, a first series of membranes was placed in a vacuum oven at 30°C for 2 hours to eliminate every trace of the solvent. This operation, however, aged the thin membrane. So, a second series of membrane was tested without the oven treatment, but ensuring a short pre-treatment of 30 min at 30°C under vacuum.

A third series of samples was treated at 120°C for 2 hours under vacuum, before the permeability tests, to accelerate the ageing process and to study the effect of the temperature in the range 30–60°C on the gas transport properties of the membranes. This thermal annealing allows to study the activation energy of the permeation process, without the effect of thermally-induced ageing during permeation tests at higher temperatures.

In the end, we fabricated and tested for gas permeability 7 samples of the material PTMSP, 5 samples of the material PTMSP/G and 7 samples of the materials PTMSP/GO, as reported in Table 1.
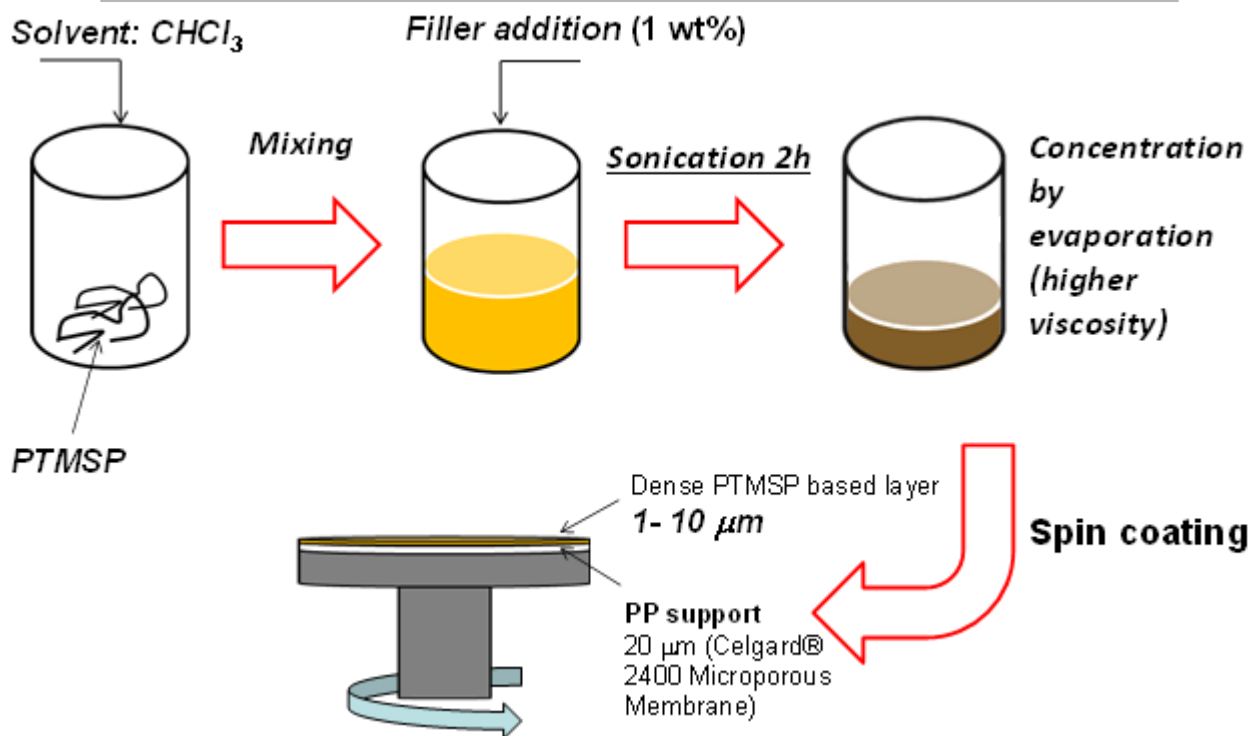
Figure 1: Preparation of thin film composite membranes with PTMSP/G and PTMSP/GO

2.3. SEM Images

The thickness of thin membranes was measured by scanning electron microscope technique (SEM, FEI XL20) after metal coating of the specimens surfaces, that allows to observe clear images with high resolution, in the order of 30-40 nm. The images are thus focused on the cross section of thin film composite membranes for thickness evaluation, but also allow to detect the presence of micrometric defects on the film surface. Figure 2 shows two different magnifications of a pure PTMSP layer coated over the porous PP support. It is clear, especially from Figure 2b, that the spin coating technique allows to obtain smooth surfaces with a homogenous appearance, although the thickness, as expected, may vary over quite a wide interval.

Also the composite films based on PTMSP/G and PTMSP/GO are pinhole-free. Figure 3a shows a thin layer of PTMSP/G composite over the porous PP support, where no pinholes are visible. Figure

8

3b presents a similar thin film composite membrane of PTMSP/GO over the PP support, where

some shear-induced stripes are visible, which indicate the liquid streamlines.

(a)

(b)
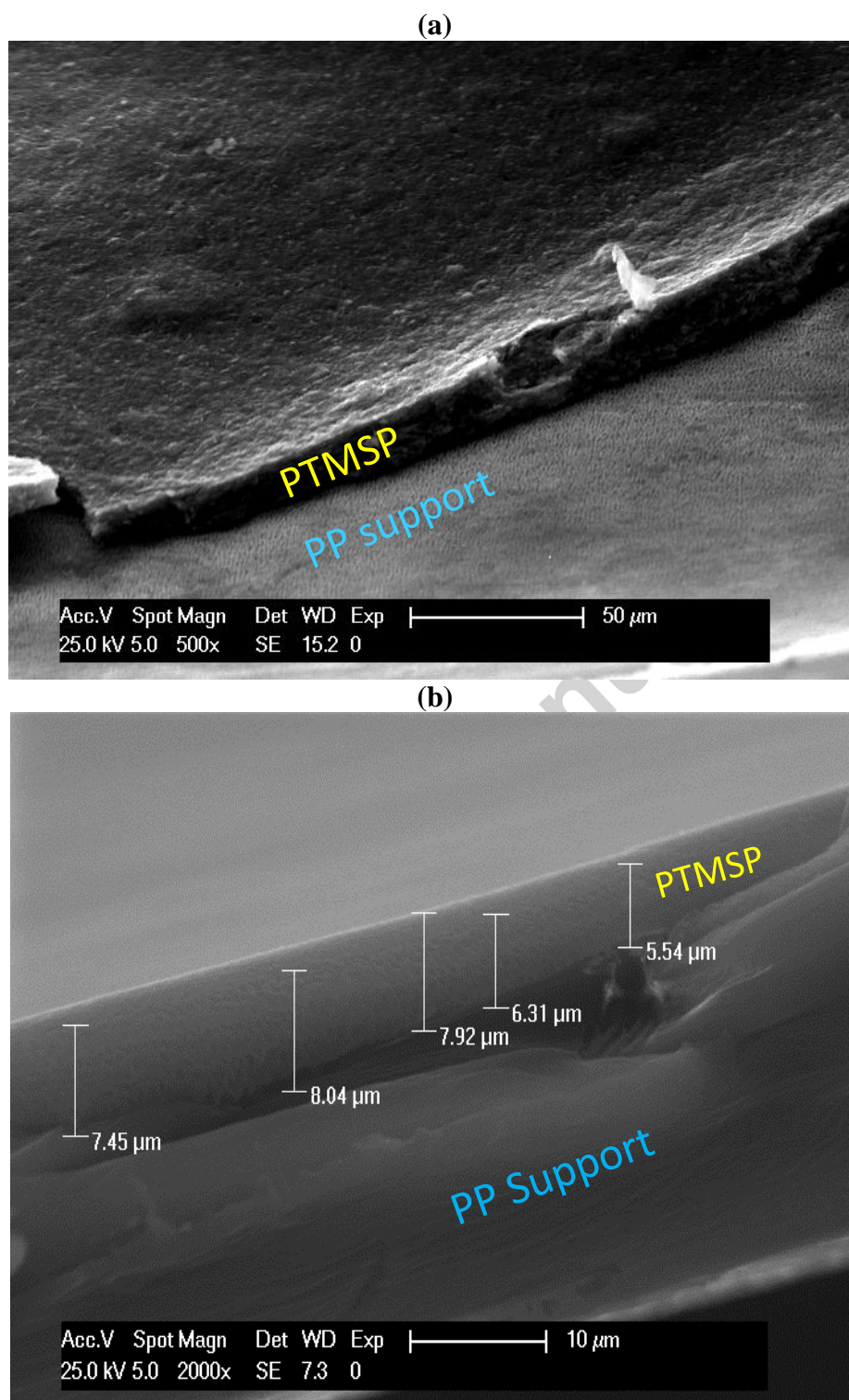
Figure 2: Cross section of a PTMSP thin film over a microporous polypropylene support (a) and example of thickness estimation during SEM scanning (b)

(a)

(b)
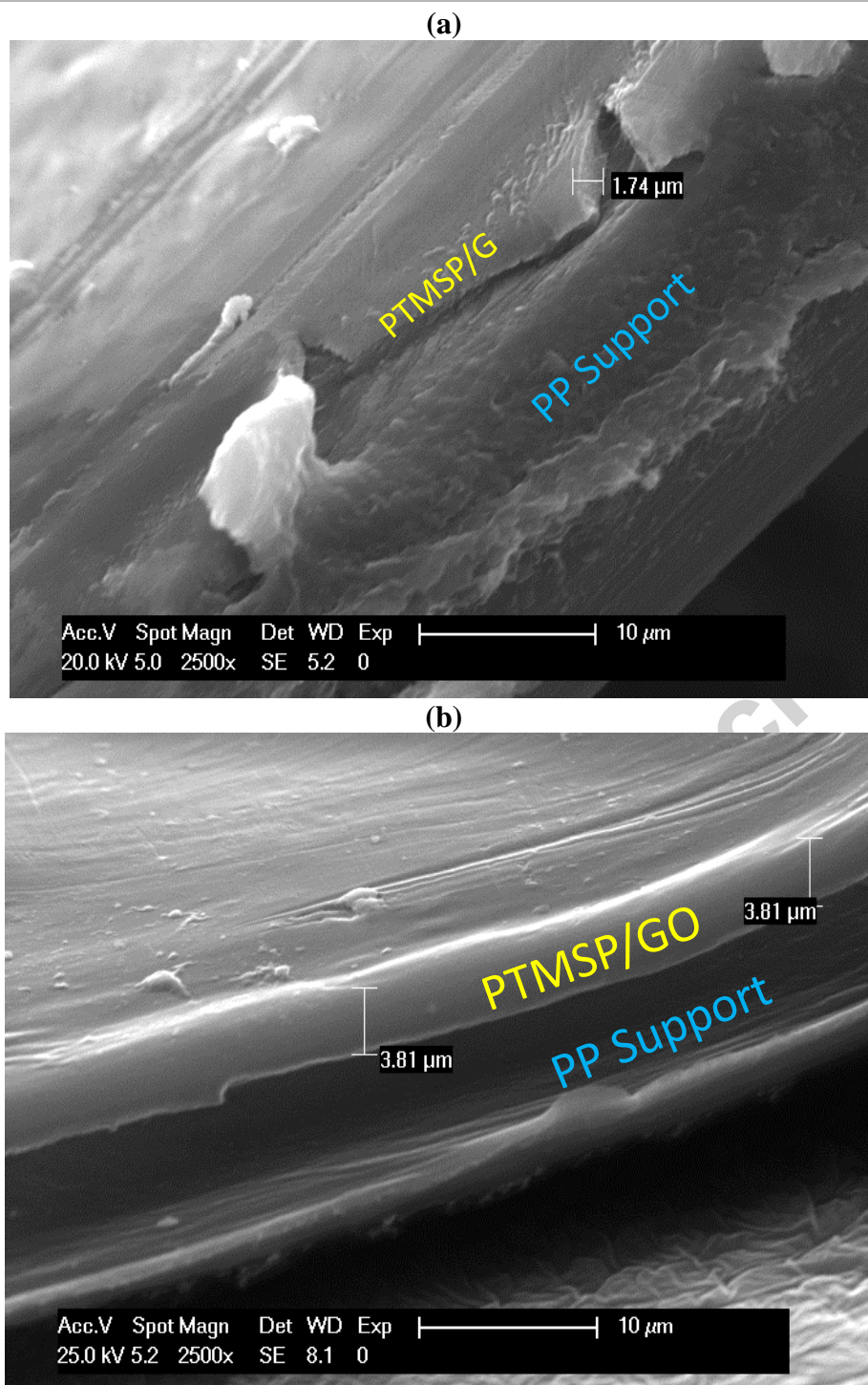
Figure 3: Cross section of a thin film composite membrane of a) PTMSP/G and b) PTMSP/GO thin films over a microporous polypropylene support

Based on SEM pictures of different points of the various membranes, we were able to measure the average thicknesses of the thin films of PTMSP, PTMSP/G and PTMSP/GO obtained, that are reported in Table 1, together with the standard deviation. Values are averaged over a minimum of 5 points for each sample.

Table 1: Thickness of the membranes produced and tested for gas permeability (μm)

PTMSP	Treatment	PTMSP/G	Treatment	PTMSP/GO	Treatment
7.0±1.0	30°C 30 min vacuum	6.1±0.4	30°C 30 min vacuum	3.2±0.6	30°C 30 min vacuum
5.7±1.8	30°C 30 min vacuum	2.4±1.2	30°C 30 min vacuum	2.6±0.7	30°C 30 min vacuum
4.9±0.3	30°C 30 min vacuum	2.1±1.0	30°C 30 min vacuum	1.8±0.4	30°C 30 min vacuum
1.6±0.5	30°C 30 min vacuum	1.5±0.4	30°C 30 min vacuum	1.7±0.2	30°C 30 min vacuum
4.0±0.4	30°C 30 min vacuum	2.3±1.0	120°C 2 h vacuum	1.6±0.3	30°C 30 min vacuum
2.6±0.9	30°C 30 min vacuum			6.2±1.0	30°C 30 min vacuum
2.0±0.9	120°C 2 h vacuum			1.6±0.8	120°C 2h vacuum

2.3. Permeability tests

The permeability was measured with a closed volume, variable pressure permeometer described in previous works, by applying an upstream pressure of about 1.3 bar and vacuum on the downstream side.[47] The pure gas permeability at steady state (P_i) can be calculated from equation 1, in which $\left.\dfrac{dp_i}{dt}\right|_{s.s.}$ is the slope of pressure versus time curve at steady state, V_d is the calibrated downstream volume, R is the universal gas constant, T is the system temperature, A is the membrane area, l is the thickness of the sample and $\left(p_i^{up} - p_i^{down}\right)$ is the gas pressure difference across the membrane film.

$$P_i = \left.\frac{dp_i}{dt}\right|_{s.s.} \frac{V_d}{RTA\left(p_i^{up} - p_i^{down}\right)} l \tag{1}$$

The temperature of the apparatus was 30°C for the first and second series sample, whereas for the third series it was used a raising temperature: 30°C - 45°C - 60°C. The permeability test were carried out following the swelling induced by the tested gas, from the lower to the higher: (1) He, (2) N_2, (3) CH_4, and (4) CO_2.

The value of permeance (permeability/thickness) calculated with the apparatus used in this work is affected by an error of ±5%, that is mainly due to uncertainty on the calibrated downstream volume,

11

while the error on the pressure reading is negligible. The permeability value is also affected by the uncertainty on the membrane thickness, which depends on the sample considered. The error on ideal selectivity of a single sample is negligible, because such value is unaffected by downstream volume, permeation area and membrane thickness values as is clear from equation 1. The same consideration holds true for the values of the ratio of current Permeability versus initial Permeability, evaluated on one same sample, reported in the graphs displaying ageing. In such cases, the values reduce to ratios between pressures, which are considered negligible.

3. Results and discussion

3.1. Study of initial permeability and comparison with thick films

The selective polymeric layer of thin membranes obtained with spin coating technique was measured with SEM (Table 1).

It is difficult to capture the initial permeability at "time zero" for thin membranes, because the macromolecular relaxation starts immediately, and its rate depends on films thickness. In particular in this work, according to other works related to physical ageing in thin films [20, 21] the initial permeability was recorded 30 minutes after film solidification. This choice is also driven by the fact that it is necessary to pull the samples under vacuum for a fixed time to ensure complete solvent removal. In these conditions, the initial gas permeability of PTMSP thin films of 7 μm thickness matches very well the values measured on 115 μm thick self-supported membranes of pure PTMSP (Figure 4: Gas permeability at 30°C of thin (7 μm) and thick [42] (115 μm) PTMSP films.
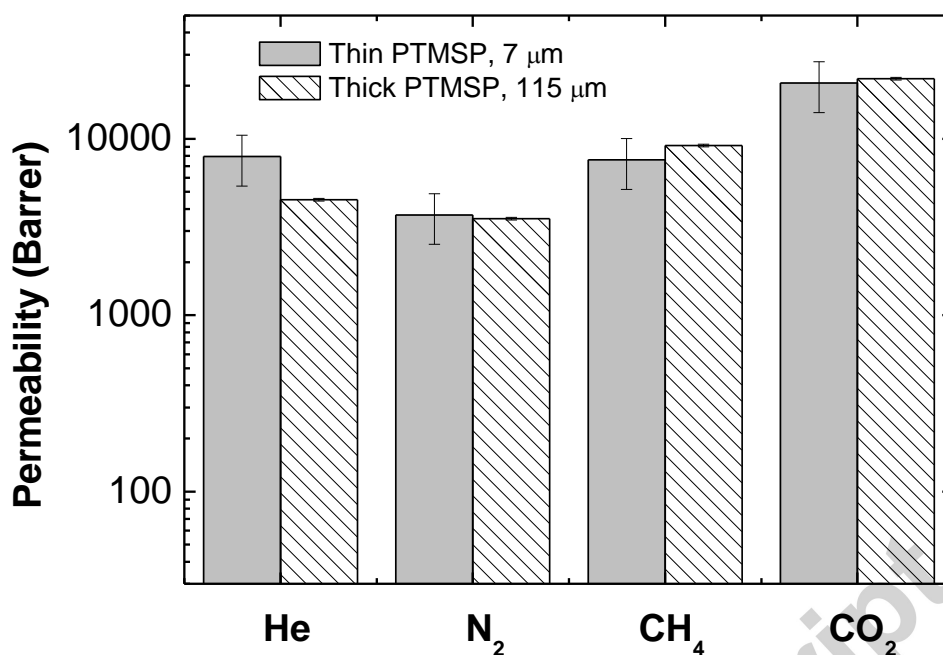
). [42]

12

Figure 4: Gas permeability at 30°C of thin (7 μm) and thick [42] (115 μm) PTMSP films.

When the composite films are considered, the comparison between thin and thick samples becomes more complicated, as there is a certain variability of the samples properties, even for samples with the same thickness, due to the different distribution and orientation of the graphene nanoplatelets in the membranes. In **Figure 5** we report a comparison between the properties of composite thin PTSMP films, from the present work, and those of thick composite PTMSP films, from our previous work.[42] The data, in particular, highlight the effect of graphene addition onto the PTMSP permeability (reported in **Figure 4**: Gas permeability at 30°C of thin (7 μm) and thick [42] (115 μm) PTMSP films.

), in terms of relative permeability variation. The data are plotted, for the various graphene types, as a function of the size of the permeating gas molecule, expressed by its kinetic diameter. The aim of such plot is to verify whether in thick and thin samples the same filler yields the same effect on the permeability, for a gas of given size.

First, from such plot one can observe that, in both thin and thick samples, the addition of GO produces a slight but detectable increase of the membrane permeability, limited to below 10%, and do not show a monotonous trend with the gas molecule size. When graphene (G) is added, both types of membranes experience a depression of gas permeability, which can be as high as -20%. Both thin and thick samples indicate that the graphene-induced decrease of permeability is larger for the smaller gas molecules (He), and smaller for the larger molecules (CH₄). The previous data [42] obtained on a different grade of graphene (G II), with a lower aspect ratio, indicate that such filler induces a strong reduction of permeability on thick samples. Moreover, such graphenic structures are thicker than the ones in this study, and they may cause defects when incorporated into thin films. Therefore, we decided not to use such filler to produce the thin membranes studied in this work.
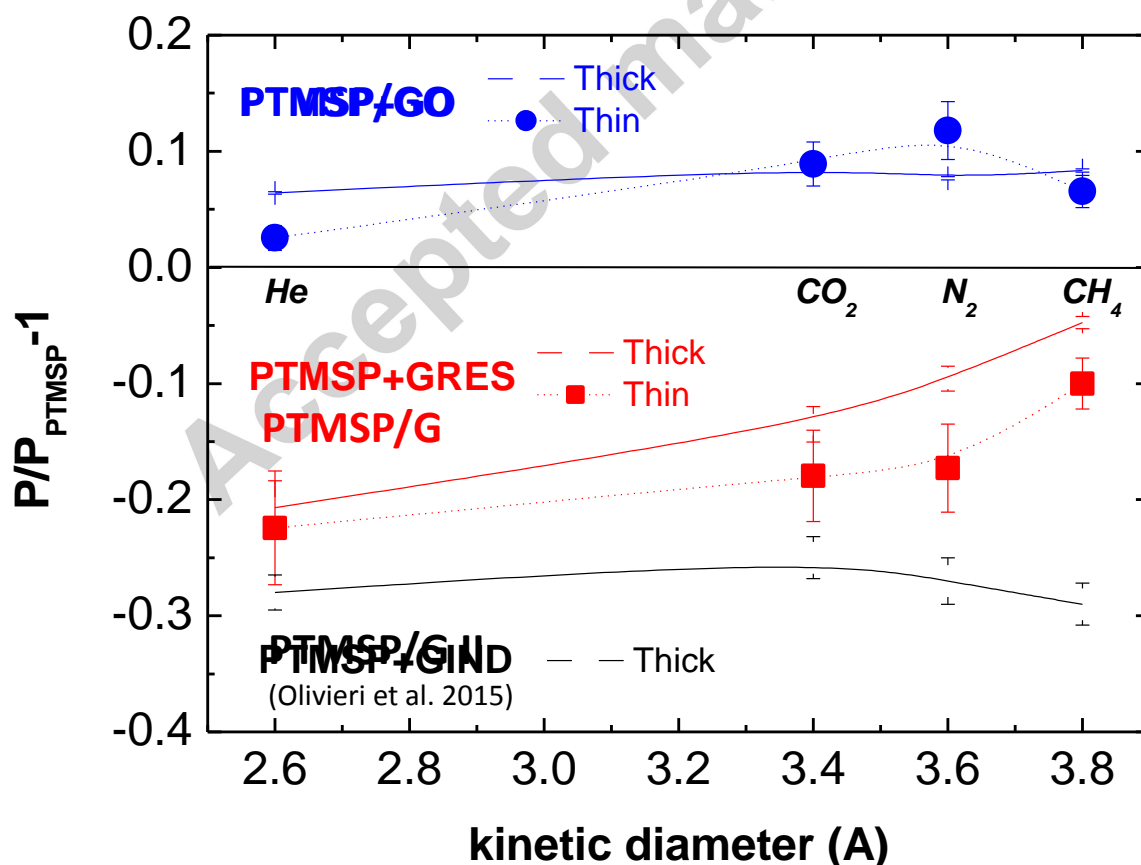

Figure 5: Effect of filler addition on initial PTMSP permeability, as a function of gas kinetic

diameter, at 30°C. Data for PTMSP/G (2.4 μm thick sample) and PTMSP/GO (6.2 μm thick sample) from this work, obtained on thin film composite membranes. Data for PTMSP/G, PTMSP/GO and PTMSP/G II from Olivieri et al.[42] obtained on thick, self-standing membranes.

Therefore, as far as the initial gas permeability is concerned, thick and thin membranes show the same trend of gas permeability, suggesting that thickness does not affect the nature of permeation trough the polymer, neither the filler effect. Also, the data indicate that composite thin membranes are not defective and that the graphenic platelets align in a similar way during the spin coating process, as they do during conventional solvent casting.

3.2. Study of ageing and comparison with thick films

Ageing is a phenomenon that affects the glassy polymers and is due to the reduction of fractional free volume (FFV) with time, which is accompanied by a parallel decay of gas permeability. The mechanism through which ageing occurs, its exact kinetics, and dependence on macromolecular parameters are still object of debate. One commonly accepted fact is that ageing rate is strictly connected to film thickness, below a threshold thickness value. [17–21] In such thickness range, which depends on the polymer type, thin films age more rapidly than thicker ones. This phenomenon was attributed to the fact that ageing is associated to a diffusive type of mechanism, i.e. by diffusion of free volume domains from the bulk to the interface of the film, and is thus strongly dependent on film thickness for thin films. Plus, the solvent evaporation rate is usually high during the formation of thin films, and the fractional free volume entrapped in the thin films is probably less stable than the one entrapped in thick ones.

In polymers characterized by a large free volume, such as PTMSP, the rate of permeability decay is a function of the gas type, according to a phenomenon known as selective ageing. [23] This is due to the fact that the reduction of free volume has different effects on different gases, but also to the fact that different sizes of "holes" may have a different depletion kinetics.

15

The thickness of polymeric layers studied in this work varied from 1 to 7 μm, a range in which the properties of PTMSP-based thin films are thickness-dependent. This is proven by the data reported in **Figure 6**, which shows the relative permeability decrease of the four different gases inspected in PTMSP films of 115 μm (self-supported) and thin films of PTMSP (2, 4, 5 and 7 μm) supported on PP. For all the gases inspected the ageing rate increases monotonically with decreasing film thickness.

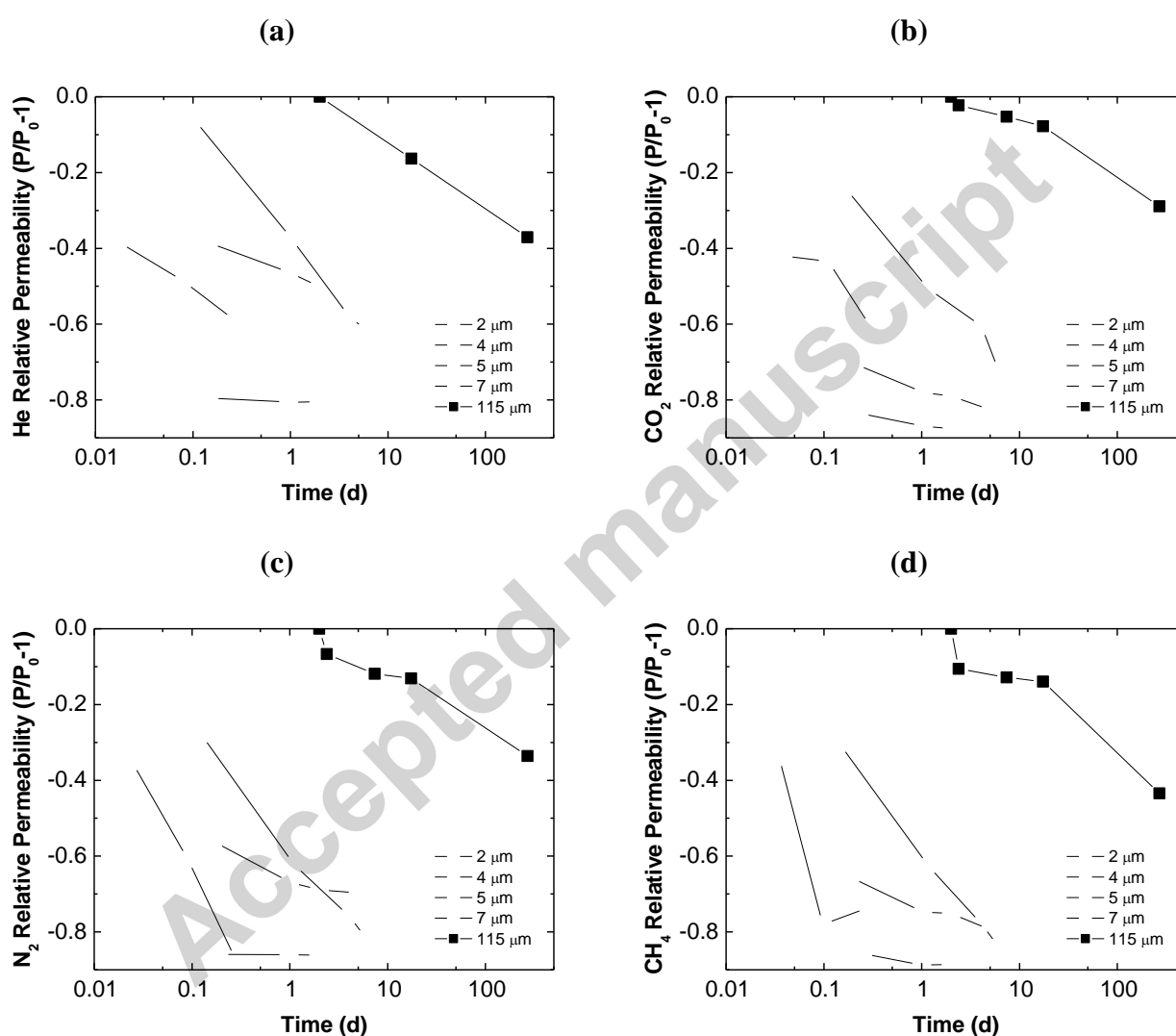**(a)**

(b)

(c)

(d)

Figure 6: physical ageing of PTMSP of different thicknesses tracked via (a) He, (b) CO_2, (c) N_2 and (d) CH_4 permeability decay versus time (days).

Therefore, to assess the effect of graphene addition on the physical ageing of thin PTMSP samples, one should consider samples of similar thickness. This comparison is presented in **Figure 7**:

16

Permeability decay at 30°C versus time for the penetrants a) He, b) CO2, c) N2, d) CH4 in thin film composite membranes of similar thickness: PTMSP (average thickness=1.6 μm); PTMSP/GO (average thickness=1.8 μm); PTMSP/G (average thickness=1.5 μm)

: three samples are considered, namely PTMSP (average thickness=1.6 μm), PTMSP/GO (average thickness=1.8 μm), PTMSP/G (average thickness=1.5 μm). The data are reported for the various gases at 30°C and indicate that the sample containing graphenic fillers are those characterized by the higher stability with respect to ageing, followed by samples containing GO, and by pure PTMSP.

Such data indicate very clearly the beneficial effect of adding graphenic compounds on the ageing: the mechanism that was observed on thick samples is thus reproduced also in thin films. Also in this case, the stabilizing effect of graphene and graphene oxide seems to be due to the reduction of diffusion of free volume pockets inside PTMSP films, as graphenic nanoplatelets acts like barriers to polymer rearrangement. The graphene is more effective than GO in reducing ageing, possibly because it has a more regular and rigid structure, composed by flat, less-defective plates. Accordingly to previous results on thick films [42], it can also be observed that the same state of ageing induces higher permeability decays in the case of CO_2 and CH_4, which are characterized by rather high initial permeability in PTMSP (21900 and 9200 Barrer, respectively), and lower decreases for N_2 and He, which show lower initial permeability in the same polymer (6700 and 3500 respectively).

(a)   (b)

17
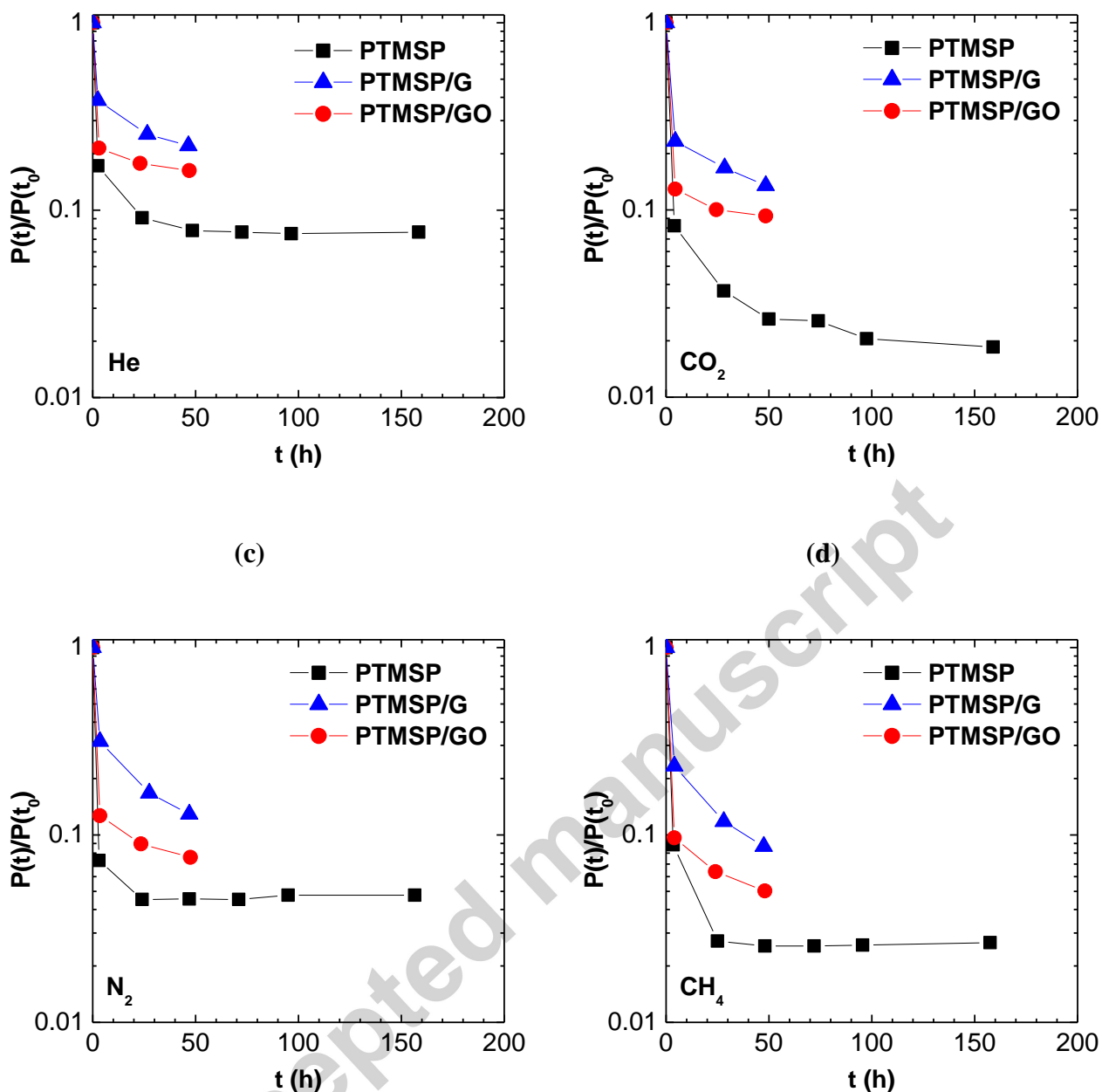
Figure 7: Permeability decay at 30°C versus time for the penetrants a) He, b) CO_2, c) N_2, d) CH_4 in thin film composite membranes of similar thickness: PTMSP (average thickness=1.6 μm); PTMSP/GO (average thickness=1.8 μm); PTMSP/G (average thickness=1.5 μm)

3.3. Modeling ageing

In order to take into account all the data obtained on thin films of different thicknesses, the following correlation between permeability decay and reduced time proposed by Huang and Paul [19] has been adopted in this study, as reported in Equation (2).

18

$$\frac{P}{P_0} = k \left(\frac{l^2}{t}\right)^n \qquad\qquad (2)$$

In particular, the authors observed that, when reported as a function of the ratio between time and squared film thickness, the data relative to different samples fall on a single masterplot. Such trend confirms the assumption that ageing is associated to a diffusive mechanism of free volume domains across the thickness of the sample.

Data of permeability decay versus time of 6 samples of thin PTMSP ranging between 1.0 and 5.0 micrometers, of 5 films of PTMSP/GO varying between 1.6 and 3.4 μm, and 3 films of PTMSP/G between 2.4 and 6.1 μm are reported in **Figure 8**: Permeability decay versus $t/l2$ for the penetrants (a) He, (b) CO2, (c) N2, (d) CH4 in the various thin film composite membranes inspected at 30°C.

as a function of t/l^2, for the various gases. Despite the scattering, the data, once fitted with the correlation represented by Equation (2), exhibit a quite regular trend, which can be analysed by comparing the values of the exponent n for the various gases and the various samples, as well as the correlation coefficient R^2, which is a measure of the accuracy of the correlation. In particular the higher the scattering of the data due to experimental error, the smaller the value of R^2. Obviously, the value of n indicates the ageing rate and can be used to quantify the stabilizing effect of filler on the membrane. Such parameters are reported in **Table 2**. The error on the value of n was estimated considering the error on thickness, which affects the values on the x-axis of Figure 8. It can be seen that the reduction of the ageing rate is particularly effective in the case of graphene, and it can be as high as 40%. In Figure 9, the values of the ageing rate, i.e. the exponent **n** of Equation (2), are quantitatively reported as a function of the gas critical temperature, for the various thin membranes inspected. The ageing rate is higher for the more permeable penetrants, which are also the more condensable ones, i.e. the ones with the higher critical temperature. In conclusion, the experimental data show that the addition of graphene oxide and graphene lowers significantly the aging rate of all tested gases.

19

(a)

(b)

(c)

(d)

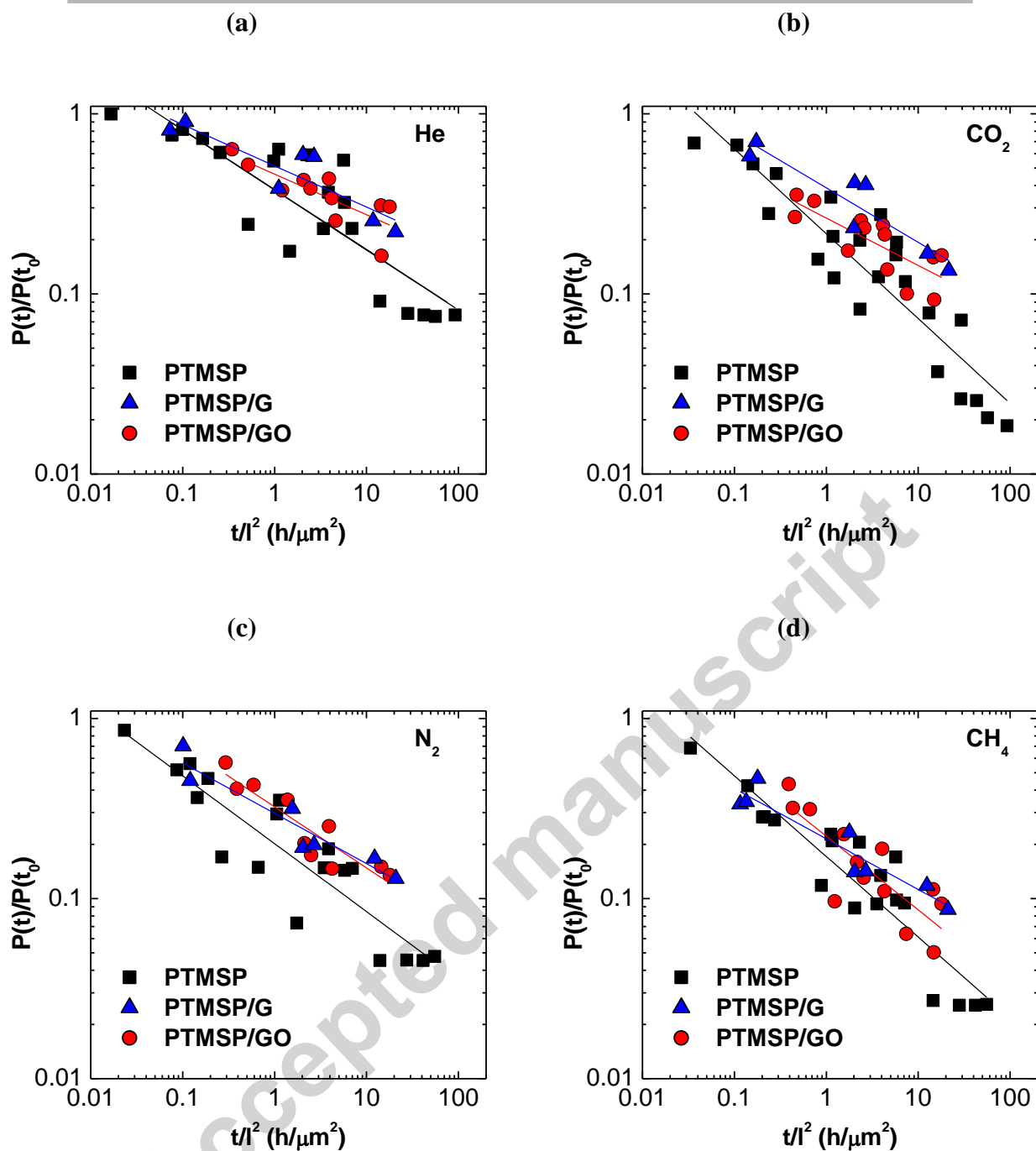**Figure 8**: Permeability decay versus t/l^2 for the penetrants (a) He, (b) CO_2, (c) N_2, (d) CH_4 in the various thin film composite membranes inspected at 30°C.

Table 2 values of exponent n and of the correlation coefficient of equation (2) at 30°C

Gas	Membrane	n	R^2
He	PTMSP	$0.333 \pm 3\%$	0.745
	PTMSP/GO	$0.226 \pm 5\%$	0.658

	PTMSP/G	$0.229 \pm 8\%$	0.806
CO_2	PTMSP	$0.471 \pm 6\%$	0.836
	PTMSP/GO	$0.335 \pm 4\%$	0.585
	PTMSP/G	$0.303 \pm 15\%$	0.856
N_2	PTMSP	$0.377 \pm 4\%$	0.820
	PTMSP/GO	$0.339 \pm 4\%$	0.840
	PTMSP/G	$0.280 \pm 4\%$	0.910
CH_4	PTMSP	$0.448 \pm 2\%$	0.863
	PTMSP/GO	$0.409 \pm 4\%$	0.695
	PTMSP/G	$0.280 \pm 1\%$	0.897
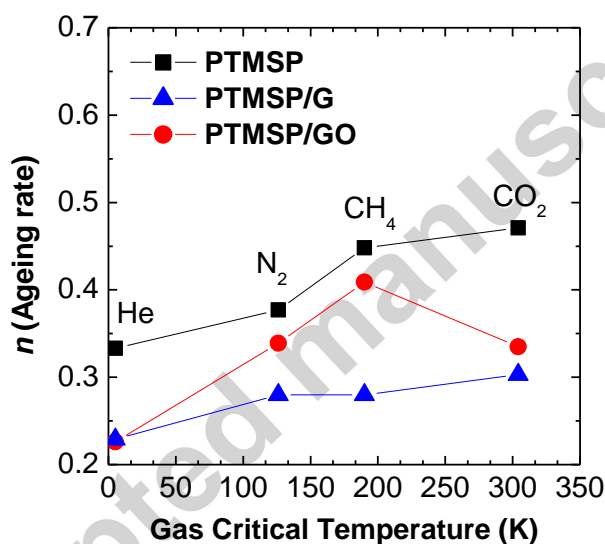
Figure 9: Correlation between ageing rate n and gas critical temperature for the various membranes inspected at 30°C.

The correlation parameters reported in Table 2 allow also to estimate the ideal selectivity of the various samples and its evolution with time. In **Figure 10**: a) CO2/N2 and b) CO2/He selectivity as a function of $t/l2$ for the various membrames inspected at 30°C

the values of selectivity for two representative couples, namely CO_2/N_2 and CO_2/He, versus the reduced time t/l^2 are reported. As it can be seen, the samples loaded with graphene oxide and, more significantly those loaded with graphene, have a higher and more stable value of selectivity with

time.

It must be noticed that the curves in Figure 10 are only partially representative of the real experimental behavior, because they were calculated with the correlation parameters of Table 2, which are affected by errors. In particular, according to the respective R^2 values, one can consider the curve relative to PTMSP/G to be the more reliable, and the curve relative to PTMSP/GO to be the less reliable. Considering the errors on the values on n reported in Table 1, the differences between the curves of PTMSP and PTMSP/GO are not significant in the majority of the time range inspected

(a)   **(b)**

Figure 10: a) CO_2/N_2 and b) CO_2/He selectivity as a function of t/l^2 for the various membrames inspected at 30°C

3.4. Effect of temperature

It is well known that temperature affects permeability by acting on both gas diffusivity and solubility in the polymeric matrix. While solubility decreases with increasing temperature, since the sorption process is exothermic, the diffusivity increases with it. Generally, the effect of diffusivity prevails, so that permeability increases with temperature, albeit with different slopes for the

different gases. Thus, the permeation is a thermally activated process which has a positive activation energy, whose value depends on the gas and polymer type. Usually, gases like CO_2, which are characterized by a large solubility, have small activation energy values for permeation. Also, polymers characterized by a high free volume have small values of activation energy. As a consequence, the selective behaviour of polymers like PTMSP may change with increasing temperature: at room temperature PTMSP is a solubility-controlled membrane, with a CO_2/H_2 and CO_2/He selectivity slightly higher than unity. At higher temperatures, where diffusivity is enhanced and solubility is depressed, the polymer may become size selective. This was proven for the H_2/CO_2 separation, for which Merkel observed an inversion in the H_2/CO_2 of selectivity at a temperature of about 120°C. [48]

In the case of high free volume glassy polymers, like PTMSP, increasing the temperature also has the effects of accelerating the ageing, thus reducing the permeability. As a result of this combination of effects, namely the low activation energy of permeation of high free volume polymers, and their thermally-induced annealing, in PTMSP, one can observe negative activation energy values. [48-49]

In the present work, in order to reduce the effect of thermal annealing on the study of activation energy, the approach of annealing the samples before studying the temperature effects was taken.

Figure 11: a)Effect of thermal annealing at 120°C for 2h on the He/CO2 separation performance of PTMSP-based thin membranes; b) effect of temperature increase, from 30 to 60°C, on the He/CO2 separation performance of annealed PTMSP-based thin membranes.

a shows, in a He/CO_2 selectivity vs. He permeability plot, the effect of thermal annealing the thin films of PTMSP and related mixed matrix films at 120°C for 2 h under vacuum. As it can be seen, such treatment lowers the permeability, while slightly enhancing the selectivity. In particular, for PTMSP-GO based samples this treatment changes the behaviour from CO_2-selective to He-

selective. Such effect could also be due to the loss of some oxygen groups of GO, induced by the annealing, which reduces the CO_2 sorption capacity of the material.

Once annealed, the effect of the temperature increase from 30 to 60°C was studied and reported in **Figure 11**: a)Effect of thermal annealing at 120°C for 2h on the He/CO2 separation performance of PTMSP-based thin membranes; b) effect of temperature increase, from 30 to 60°C, on the He/CO2 separation performance of annealed PTMSP-based thin membranes.

 b. In particular, it is seen that increasing the temperature has the effect of enhancing both the He/CO_2 selectivity and He permeability of PTMSP and PTMSP/G samples, while the behaviour of PTMSP/GO samples is not monotonous and deserves further analysis.

From the data of PTMSP and PTMSP/G, one can extrapolate the behavior at higher temperatures. If extrapolated to 200°C according to an Arrhenius type of law, the PTMSP/G shows a hypothetical permeability of around 9000 Barrer for He, and a selectivity of about 10 for He/CO_2.
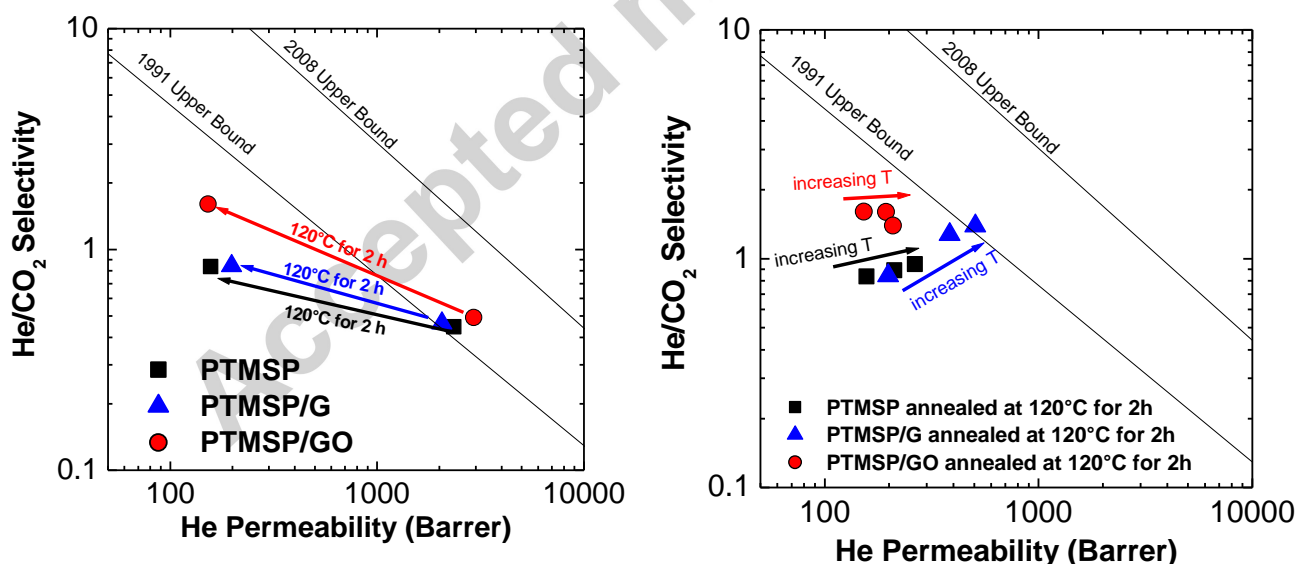

Figure 11: a)Effect of thermal annealing at 120°C for 2h on the He/CO_2 separation performance of PTMSP-based thin membranes; b) effect of temperature increase, from 30 to 60°C, on the He/CO_2 separation performance of annealed PTMSP-based thin membranes.

Conclusions

Thin composite membranes based on PTMSP and small loadings (1 wt%) of few layer graphene and graphene oxide were fabricated by spin coating. Despite the large lateral size of the graphenic fillers, membranes with thickness between 1 and 7 μm were produced without defects, indicating that graphenic platelets align parallel to the horizontal surface of the film during coating, and that their production can be potentially scaled up.

The membranes were analysed for He, N_2, CH_4 and CO_2 permeability at 30, 45 and 60°C. The effect of the graphene and GO addition to the PTMSP, in thin films, is qualitatively similar to the one obtained in thicker films studied in a previous work. [42] Indeed, the addition of GO slightly enhances the permeability of PTMSP towards all gases, while the addition of graphene reduces the permeability, with factors that increase with decreasing the size of the penetrant.

The ageing was studied on several samples, by monitoring the decay of gas permeability with time. The aging rate of thin films is inversely related to the film thickness, and the decay of gas permeability is faster for gases with higher critical temperature. The ageing data, fitted with a power law, indicate that the *n* exponent, representative of the ageing rate, decreases significantly with the addition of either graphene or graphene oxide to PTMSP, by factors as high as 40%. This behaviour confirms what observed in thicker membranes, and indicates that the graphenic fillers slow down the aging of PTMSP, by acting as physical barriers to the rearrangement of the polymer chains. Such effect could favour the industrial application of PTMSP and other high free volume glassy materials, which have poor stability.

An accelerated ageing, induced via thermal annealing at 120°C for 2h, drastically lowers the permeability to all gases of all membranes, and slightly enhances the selectivity, by reducing the free volume. In the case of the PTMSP/GO membrane, the behavior changes from CO_2-selective to He-selective after the treatment. The effect of temperature on gas transport in the membranes was determined in the range from 30 to 60°C on annealed samples. Increasing the temperature has the

effect of making the membranes He-selective. Both the He permeability and the He/CO$_2$ selectivity increase with temperature, especially in the case of the membrane loaded with graphene, which show interesting values for the high temperature separation of He/CO$_2$ mixture.

Acknowledgements

REFERENCES

[1]   L. M. Robeson, The upper bound revisited. J. Membr. Sci. 320 (2008) 390.

[2]   C.M. Zimmerman, A. Singh, W.J. Koros, W.J. Tailoring Mixed Matrix Composite Membranes For Gas Separations. J. Membr. Sci. 137 (1997) 145–154.

[3]   R. Mahajan., W. J. Koros, Factors Controlling Successful Formation of Mixed-Matrix Gas Separation Materials. Ind. Eng. Chem. Res. 2000, 39, 2692–2696.

[4]   D.Q. Vu, W. J. Koros, S. J. Miller, Mixed matrix membranes using carbon molecular sieves I. Preparation and experimental results, J. Membr. Sci. 211 (2003) 311–334.

[5]   I. Pinnau, Z. He, Filled superglassy membrane. US patent 6,316,684.

[6]   T. C. Merkel, Z. He, I. Pinnau, B. D. Freeman, P Meakin, A. J. Hill, Effect of Nanoparticles on Gas Sorption and Transport in Poly(1-trimethylsilyl-1-propyne). Macromolecules 36 (2003) 6844–6855.

[7]   T. C. Merkel, Z. He, I. Pinnau, B. D. Freeman, P. Meakin, A. J. Hill, Sorption and Transport in Poly (2,2-bis(trifluoromethyl)-4,5-difluoro-1,3-dioxole-co-tetrafluoroethylene) Containing Nanoscale Fumed Silica, Macromolecules 36 (2003) 8406–8414.

[8]   T. C. Merkel, B. D. Freeman, R. J. Spontak, Z. He, I. Pinnau, P. Meakin, A. J. Hill, Sorption, Transport, and Structural Evidence for Enhanced Free Volume in Poly(4-methyl-2-pentyne)/Fumed Silica Nanocomposite Membranes, Chem. Mater. 15 (2003) 109–123.

[9]   J. Ahn, W. J. Chung, I. Pinnau, J. Song, N. Du, G. P. Robertson, M. D. Guiver, Gas transport behavior of mixed-matrix membranes composed of silica nanoparticles in a polymer of intrinsic microporosity (PIM-1), J. Membr. Sci. 346 (2010) 280–287.

[10]   J. Ahn, W. J. Chung, I. Pinnau, M. D. Guiver, Polysulfone/silica nanoparticle mixed-matrix membranes for gas separation, J. Membr. Sci. 314 (2008) 123–133.

[11]   M. C. Ferrari, M. Galizia, M. G. De Angelis, G. C. Sarti, Gas and Vapor Transport in Mixed Matrix Membranes Based on Amorphous Teflon AF1600 and AF2400 and Fumed Silica, Ind. Eng. Chem. Res. 49 (2010) 11920–11935.

[12]   M. Galizia, M. G. De Angelis, M. Messori, G. C. Sarti, Mass transport in hybrid PTMSP/Silica membranes, Ind. Eng. Chem Res. 53 (2014) 9243–9255.

[13]   M. G. De Angelis, G. C. Sarti, Solubility and Diffusivity of Gases in Mixed Matrix Membranes Containing Hydrophobic Fumed Silica: Correlations and Predictions Based on the NELF Model, Ind. Eng. Chem Res. 47 (2008) 5214–5226.

[14]   T. C. Merkel, B. D. Freeman, R. J. Spontak, Z. He, I. Pinnau, P. Meakin, A. J. Hill, Ultrapermeable, Reverse-Selective Nanocomposite Membranes, Science 296 (2002)519–522.

[15]   M. G. De Angelis, R. Gaddoni, G. C. Sarti, Gas Solubility, Diffusivity, Permeability, and Selectivity in Mixed Matrix Membranes Based on PIM-1 and Fumed Silica, Ind. Eng. Chem. Res. 52 (2013) 10506–10520.

[16]   M. G. De Angelis, G. C. Sarti, Gas sorption and permeation in mixed matrix membranes based on glassy polymers and silica nanoparticles, Curr. Opin. Chem. Eng. 1 (2012) 148–155.

[17]   J. M. Hutchinson, Physical aging of polymers. Prog. Polym. Sci. 20 (1995) 703–760.

[18]   Struik, L. C. E. Physical Ageing in Amophous Polymers and Other Materials; Elsevier: New York, 1978.

[19]   Y. Huang, D. Paul, Physical aging of thin glassy polymer films monitored by gas permeability, Polymer 45 (2004) 8377–8393.

[20]   Y. Huang, X. Wang, D. Paul, Physical aging of thin glassy polymer films: Free volume interpretation, J. Membrane Sci. 277 (2006) 219-229.

[21]   K. D. Dorkenoo, P.H. Pfromm, Accelerated Physical Aging of Thin Poly[1-(trimethylsilyl)-1-propyne] films, Macromolecules 33 (2000) 3747–3751.

[22]   T. Koschine, K. Rätzke1, F. Faupel, M. Munir Khan, T. Emmler, V. Filiz, V. Abetz, L. Ravelli, W. Egger, Correlation of Gas Permeation and Free Volume in New and used High Free Volume Thin Film Composite Membranes, J. Polymer Sci. Part B: Polym. Phys. 53 (2015) 213–217.

[23]   C. Hon Lau, P. Tien Nguyen, M. R. Hill, A. W. Thornton, K. Konstas, C. M. Doherty, R. J. Mulder, L. Bourgeois, A. C. Y. Liu, D. J. Sprouster, J. P. Sullivan, T. J. Bastow, A. J. Hill, D. L. Gin, R. D. Noble, Ending Aging in Super Glassy Polymer Membranes, Angew. Chem. Int. Ed. 53 (2014) 5322–5326.

[24]   S. D. Kelman, B. W. Rowe, C. W. Bielawski, S. J. Pas, A. J. Hill, D. R. Paul, B. D. Freeman, Crosslinking poly(1-(trimethylsilyl)-1-propyne) and its effect on physical stability, J. Membr. Sci. 320 (2008) 123–134.

[25]   S. Matteucci, V. A. Kusuma, D. Sanders, S. Swinnea, B. D. Freeman, Gas transport in TiO_2 nanoparticle-filled poly (1-trimethylsilyl-1-propyne), J. Membr. Sci. 307 (2008) 196–217.

[26]   S. Matteucci, V. A. Kusuma, S. D. Kelman, B. D. Freeman, Gas transport properties of MgO filled poly(1-trimethylsilyl-1-propyne) nanocomposites, Polymer 49 (2008) 1659–1675.

[27]   H. W. Kim, H. W. Yoon, S. M. Yoon, B. M. Yoo, B. K. Ahn, Y. H. Cho, H. J. Shin, H. Yang, U. Paik, S. Kwon, J. Y. Choi, H. B. Park, Selective Gas Transport Through Few-Layered Graphene and Graphene Oxide Membranes, Science 342 (2013) 91–95.

[28]   H. Li, Z. Song, X. Zhang, Y. Huang, S. Li, Y. Mao, H. J. Ploehn, Y. Bao, M. Yu, Ultrathin, Molecular-Sieving Graphene Oxide Membranes for Selective Hydrogen Separation, Science 342 (2013) 95–98.

[29]   B. M. Yoo, J. E. Shin, H. D. Lee, H. B. Park, Graphene and graphene oxide membranes for gas separation applications, Curr. Op. Chem. Eng. 16 (2017) 39–47.

[30]   C. Sun, B.Wen, B. Bai, Recent advances in nanoporous graphene membrane for gas separation and water purification, Sci. Bull. 60 (2015) 1807-1823.

[31]   L. Huang, M. Zhang, C. Li, G. Shi, Graphene-Based Membranes for Molecular Separation, J. Phys. Chem. Lett 6 (2015) 2806−2815.

[32]   H. W. Yoon, Y. H. Cho, H. B. Park, Graphene-based membranes: status and prospects, Philos. Trans. R. Soc. A Math. Phys. Eng. Sci. 347 (2016) 20150024.

[33]   B. M. Yoo, H. J. Shin, H. W. Yoon, H. B. Park, Graphene and graphene oxide and their uses in barrier polymers, J. Appl. Polym. Sci. 131 (2013) 131, 39628–39650.

[34]   J. Zhu, J. Lim, C. H. Lee, H. I. Joh, H. Chul Kim, B. Park, N. H, You, S. Lee, Multifunctional polyimide/graphene oxide composites via in situ polymerization, J. Appl. Polym. Sci. 131 (2014) 40177–40183.

[35]   H. Kim, H. Yoon, B. Yoo, J. Park, K. Gleason, B. D. Freeman, H. Park, High performance CO_2-phylic graphene oxide membranes under wet conditions, Chem. Communications 88 (2014) 13563–13566.

[36]   J. Shen, G. Liu, K. Huang, W. Jin, K.-R. Lee, N. Xu, Membranes with Fast and Selective Gas-Transport Channels of Laminar Graphene Oxide for Efficient CO2 Capture, Angenwadte Chemie 127 (2015) 588–592.

[37]   X. Li, L. Ma, H. Zhang, S. Wang, Z. Jiang, R. Guo, H. Wu, X. Z. Cao, J. Yang, B. Wang, Synergistic effect of combining carbon nanotubes and graphene oxide in mixed matrix membranes for efficient CO_2 separation, J. Membr. Sci. 479 (2015) 1−10.

[38]   L. Zhao, C. Cheng, Yu-Fei Chen, T. Wang, Chun-Hui Du, Li-Guang Wu, Enhancement on the permeation performance of polyimide mixed matrix membranes by incorporation of graphene oxide with different oxidation degrees, Polymers advanced technologies 26 (2015) 330–337.

[39]   A. Gonciaruk, K. Althumayri, W.J. Harrison, P.M. Budd, F.R. Siperstein, PIM-1/graphene composite: A combined experimental and molecular simulation study, Microporous and Mesoporous Materials 209 (2015) 126–134.

[40]   K. Althumayri, W. J. Harrison, Y. Shin, J. M. Gardiner, C. Casiraghi, P. M. Budd, P. Bernardo, G. Clarizia, J. C. Jansen, The influence of few-layer graphene on the gas permeability of the high-free-volume polymer PIM-1, Phil. Trans. R. Soc. A 374 (2016) 20150031.

[41]   Y. Shin, E. Prestat, K.-G. Zhou, P. Gorgojo, K. Althumayri, W. Harrison, P.M. Budd, S.J. Haigh, C. Casiraghi, Synthesis and characterization of composite membranes made of graphene and polymers of intrinsic microporosity, Carbon 102 (2016) 357-366.

[42]   L. Olivieri, S. Ligi, M.G. De Angelis, G. Cucca, A. Pettinau, Effect of Graphene and Graphene Oxide Nanoplatelets on the Gas Permselectivity and Aging Behavior of Poly(trimethylsilyl propyne) (PTMSP), Ind. Eng. Chem. Res. 54 (2015) 11199 – 11211.

[43]   K. Kouroupis-Agalou, A. Liscio, E. Treossi, L. Ortolani, V. Morandi, N. M. Pugno, V. Palermo, Fragmentation and exfoliation of 2-dimensional materials: a statistical approach, Nanoscale 6 (2014) 5926-5933.

[44]   A. Liscio, K. Kouroupis-Agalou, X. D. Betriu, A. Kovtun, E. Treossi, N. M. Pugno, G. De Luca, L. Giorgini, V. Palermo, Evolution of the size and shape of 2D nanosheets during ultrasonic fragmentation, 2D Materials 4 (2017) 25017–25024.

[45]   Y. Zhang, Q. Shen, J. Hou, P. D. Sutrisna, V. Chen, Shear-aligned graphene oxide laminate/Pebax ultrathin composite hollow fiber membranes using a facile dip-coating approach, J. Mater. Chem. A, 2017, 5, 7732–7737.

[46]   R. Rea, S. Ligi, M. Christian, V. Morandi, M. Giacinti Baschetti, M.G. De Angelis, Permeability and selectivity of PPO/graphene composites as mixed matrix membranes for CO_2 capture and gas separation, Polymers 10 (2018) 129–147.

[47]   M. Minelli, M. G. De Angelis, F. Doghieri, M. Marini, M. Toselli, F. Pilati, Oxygen permeability of novel organic–inorganic coatings: I. Effects of organic–inorganic ratio and molecular weight of the organic component, Eur. Polym. J. 44 (2008) 2581–2588.

[48]   T.C. Merkel, R.P. Gupta, B.S. Turk, B.D. Freeman, Mixed-gas permeation of syngas components in poly(dimethylsiloxane) and poly(1-trimethylsilyl-1-propyne) at elevated temperatures, J. Membr. Sci. 2001, 191, 85-94.

[49]   T. Nakagawa, T. Saito, S. Asakawa, Y. Saito, Polyacetylene derivatives as membranes for gas separation, Gas Separation and Purification, 1988, 2, 3-8.

Highlights

1) Membranes of PTMSP +G, GO between 1 and 7 micrometers were produced
2) Graphene lowers the permeability of PTMSP, while GO enhances it.
3) The ageing of the PTMSP membranes is visibly reduced by addition G and GO
4) The He/CO_2 separation performance is improved by addition of G and GO
5) The activation energy of permeation was assessed on annealed samples